planar subgraph from the nonplanar or planar graph and embeds it on a plane.

0) Set $t = 0$.

1) Randomize the initial values of $Uup_{ij}(t)$ and $Udown_{ij}(t)$, where $i = 1,...,N$ and $j = 1,...,N$, in the range $-\omega$ to 0; ω is a real number.

2) Evaluate values of $Vup_{ij}(t)$ and $Vdown_{ij}(t)$ on the basis of the binary function, where $i = 1,...,N$ and $j = 1,...,N$.

$$Vup_{ij}(t) = f[Uup_{ij}(t)] = \begin{matrix} 1 \text{ if } Uup_{ij}(t) > 0 \\ 0 \quad \text{otherwise} \end{matrix} \qquad (4)$$

$$Vdown_{ij}(t) = f[Udown_{ij}(t)] = \begin{matrix} 1 \text{ if } Udown_{ij}(t) > 0 \\ 0 \quad \text{otherwise} \end{matrix} \qquad (5)$$

3) Use the motion equation (Eq. 3) to compute $\Delta Uup_{ij}(t)$ and $\Delta Udown_{ij}(t)$.

$$\begin{aligned} \Delta Uup_{ij}(t) = & \\ & -A[Vup_{ij}(t) + Vdown_{ij}(t) - C_{ij}] \\ & - B\sum_{\ell}\sum_{\substack{m \\ \ell<m}} f(\ell,i,m)f(i,m,j)\,Vup_{\ell m}(t) \\ & - B\sum_{\ell}\sum_{\substack{m \\ \ell<m}} f(i,\ell,j)f(\ell,j,m)\,Vup_{\ell m}(t) \quad (6) \end{aligned}$$

$$\begin{aligned} \Delta Udown_{ij}(t) = & \\ & -A[Vup_{ij}(t) + Vdown_{ij}(t) - C_{ij}] \\ & - B\sum_{\ell}\sum_{\substack{m \\ \ell<m}} f(\ell,i,m)f(i,m,j)\,Vdown_{\ell m}(t) \\ & - B\sum_{\ell}\sum_{\substack{m \\ \ell<m}} f(i,\ell,j)f(\ell,j,m)\,Vdown_{\ell m}(t) \quad (7) \end{aligned}$$

4) Compute $Uup_{ij}(t + 1)$ and $Udown_{ij}(t) + 1)$ on the basis of the first-order Euler method:

$$Uup_{ij}(t + 1) = Uup_{ij}(t) + \Delta Uup_{ij}(t)\Delta t \qquad (8)$$

$$Udown_{ij}(t + 1) = Udown_{ij}(t) + \Delta Udown_{ij}(t)\Delta t \qquad (9)$$

where $i = 1,...,N$ and $j = 1,...,N$.

5) Increment t by 1. If $t = T$, then terminate this procedure, otherwise go to step 2.

Consider the nonplanar graph of Jayakumar *et al.* (*2*) in Fig. 3a. The graph has 10 vertices and 22 edges. The latest experiment by Jayakumar *et al.* showed that 19 edges were chosen by their $0(N^2)$ algorithm to construct the maximal planar subgraph as shown in Fig. 3b. Remember that their algorithm does not embed the generated subgraph on a plane but chooses edges for construction of the maximal planar subgraph.

We have developed a simulator based on the proposed algorithm on a Macintosh and on an Apollo 3500 computer. When the coefficients $A = 2$ and $B = 1$ and the unit time $\Delta t = 10^{-5}$ were used for Eqs. 6 through 9, and the initial values of $Uup_{ij}(t)$ and $Udown_{ij}(t)$ were randomized in the range of $-1/10{,}000$ to 0, the state of our system converged to the global minimum in the 14th iteration. Figure 4, a and b, describes the state of the system at the first and 14th iterations. Our simulator found that the new maximal planar subgraph contains 20 edges instead of 19 edges, which contradicts the result of Jayakumar *et al.* (*2*). Table 1 shows the simulation results where several sets of the coefficients were used. It indicates that either 20 edges or 19 out of 22 edges can be consistently embedded in a single plane.

Within 0(1) time the algorithm not only generates a near-maximal planar subgraph from the nonplanar or planar graph but also embeds the subgraph on a plane. On the basis of our observations of the behavior of the simulator, the state of the system always converges to a good solution within 20 or 30 iteration steps. Another simulation result of a graph with 48 vertices and 105 edges also showed the consistency of our algorithm. The algorithm can be implemented by an $N \times N$ two-dimensional neural network array. Among N^2 neurons, only $2M$ neurons are used to obtain the solution. The detailed design of the parallel hardware is given in (*7*).

REFERENCES AND NOTES

1. M. R. Garey and D. S. Johnson, *Computers and Intractability: A Guide to the Theory of NP-Completeness* (Freeman, San Francisco, 1979).
2. R. Jayakumar *et al.*, *IEEE Trans. CAD* **8**, 3 (March 1989).
3. R. E. Tarjan, *Publication STAN-CS-244-71* (Computer Science Department, Stanford University, Stanford, CA, 1971).
4. H. Szu, in *Proceedings of the International Conference on Neural Networks* (IEEE, Piscataway, NJ, 1989), vol. 2, p. 259.
5. J. Hopfield and D. Tank, *Biol. Cybern.* **52**, 141 (1985).
6. Y. Takefuji in *Proceedings of the International Joint Conference on Neural Networks et al.*, (IEEE, Piscataway, NJ, 1989), p. 529.
7. ——— and K.-C. Lee, *CAISR Tech. Rep. TR 88-139* (Center for Automation and Intelligent Systems Research, Case Western Reserve University, Cleveland, 1988).

30 May 1989; accepted 25 July 1989

Shear Forces in Molecularly Thin Films

MARTIN SCHOEN, CHARLES L. RHYKERD, JR., DENNIS J. DIESTLER, JOHN H. CUSHMAN

Monte Carlo and molecular dynamics methods have been used to study the shearing behavior of an atomic fluid between two plane-parallel solid surfaces having the face-centered cubic (100) structure. A distorted, face-centered cubic solid can form epitaxially between surfaces that are separated by distances of one to five atomic diameters. Under these conditions a critical stress must be overcome to initiate sliding of the surfaces over one another at fixed separation, temperature, and chemical potential. As sliding begins, a layer of solid exits the space between the surfaces and the remaining layers become fluid.

IN THE LAST DECADE IT HAS BECOME feasible, if not routine, to measure directly on a molecular scale the forces between two solid surfaces separated by a film of fluid (*1–3*). When the distance h between the surfaces is in the range from one to ten "diameters" of the fluid molecule, the component of the force normal to the surfaces oscillates as a function of h, alternating between attraction and repulsion with a period approximately equal to the molecular diameter. This oscillatory character suggests that the fluid near the surfaces arranges itself in layers parallel with the surfaces and that entire layers of fluid are successively forced from the space between the surfaces as h is decreased. Statistical mechanics calculations confirm this notion.

Both Monte Carlo (*4–9*) and molecular dynamics (*10–12*) studies of model slit pores (that is, fluid confined between two plane-parallel solid walls) show that an atomic pore fluid does indeed pile up in layers parallel with the walls, whether the walls are structured or not. This "normal" ordering of the fluid is analogous to the ordering of fluid

---

M. Schoen, Universität Witten/Herdecke, Naturwissenschaftliche Fakultät, Institut für Experimentalphysik, Stockumer Strasse 10, 5810 Witten, Federal Republic of Germany.
C. L. Rhykerd, Jr., and J. H. Cushman, Department of Agronomy, Purdue University, West Lafayette, IN 47907.
D. J. Diestler, Department of Chemistry, Purdue University, West Lafayette, IN 47907.

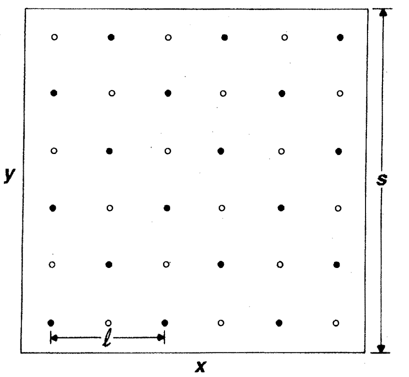

Fig. 1. Top view of the unit simulation cell. Filled circles represent atoms in lower wall 1 ($z = 0$), open circles represent atoms in upper wall 2 ($z = h$). Walls are shown fully out of registry (strain $\alpha = 0.5$).

molecules about a reference molecule in the bulk. The walls behave essentially as reference molecules of infinite radius.

Until our grand-canonical Monte Carlo studies (*8, 9*) of the prototypal structured slit pore [atomic fluid confined by face-centered cubic (fcc) (100) planes of like atoms], no clear evidence of order within the fluid layers in directions parallel with the walls, that is "transverse" order, had been reported. We discovered that, over a range of h from one to about six atomic diameters, the pore "fluid" alternately freezes and thaws as a function of h, other thermodynamic state variables (specified later) being held constant. The pore solid forms epitaxially; the successive layers are distorted fcc (100) structures. Thus, the structured walls induce freezing, even when the corresponding bulk phase is fluid. This epitaxial effect decreases with increasing h but persists indefinitely in the contact layer.

Experimental examination of the behavior of thin fluid films that are undergoing transverse movement (that is, shearing) of the solid surfaces has only begun. Dynamic shear-response measurements (*13, 14*), performed on organic liquids between atomically smooth mica sheets, show that the apparent viscosity of the fluid in molecularly thin films can be greater by up to seven orders of magnitude than that in the bulk. These measurements indicate that the solid surfaces slide past one another while separated by discrete numbers of fluid layers and that under appropriate conditions a critical shear stress S_c is required to initiate sliding. Moreover, S_c is "quantized" with the number of fluid layers, that is, S_c changes as the number of layers changes. The fact that a critical stress is required to initiate sliding suggests that the pore "fluid" has assumed a solid-like structure that must be broken down in order for sliding to occur.

We present here the results of Monte Carlo and molecular dynamics calculations that support the above interpretation of the shear measurements (*13, 14*). For simplicity, we have restricted our study to the prototypal slit pore. Each wall is composed of N_s atoms rigidly fixed in the configuration of (100) planes of the fcc lattice (see Fig. 1). The relative location of the walls in the x direction is specified by a parameter α, which relates the x coordinate of an atom in wall 2 to that of the corresponding atom in wall 1 by

$$x_2 = x_1 + \alpha\ell \qquad (1)$$

where ℓ is defined in Fig. 1. Thus, the quantity α permits us to slide the upper wall (position x_2) in the x direction while keeping the lower wall (position x_1) fixed. We shall refer to α as the registry or strain. The space between the walls is occupied by N fluid atoms identical with the wall atoms. The total potential energy of the system is taken as a sum of Lennard-Jones (12, 6) pairwise interactions

$$u(r) = 4\epsilon[(\sigma/r)^{12} - (\sigma/r)^6] \qquad (2)$$

where r is the distance between the atoms of a pair, $-\epsilon$ is the minimum of the interaction, and σ is the atomic "diameter."

In the actual measurements (*13, 14*), the walls slide by one another at a rate on the order of 10^{-9} Å/ps. It is computationally impossible to follow the motion of our model system for a real time longer than about 10^3 ps. Therefore, on the molecular scale of the computer "experiment" the walls are practically stationary. In the real experiments, the slit pore has a finite extent and the pore fluid is presumably in contact, if not in equilibrium, with the surrounding bulk fluid. In the computations we treat the pore as if it were of infinite extent by imposing periodic boundary conditions on the unit simulation cell in the x and y directions (Fig. 1). The model pore fluid is not in direct contact with the bulk fluid but is taken to be in thermodynamic equilibrium with the bulk fluid, whose thermodynamic state is specified by the chemical potential μ and absolute temperature T. Thus, μ and T for the pore fluid must equal the respective values for the bulk fluid. We must also specify the registry α and the distance h between the walls in order to determine uniquely the thermodynamic state of the pore fluid.

In certain regions of the pore's thermodynamic state space (μ, T, h, α) where the bulk phase is fluid, a solid exists in the pore. When the walls are either in registry ($\alpha = 0.0$) or out of registry ($\alpha = 0.5$), respectively, odd or even numbers of distorted fcc (100) layers of pore solid form, depending on h (*9*). We surmise that under these conditions the pore is in stable mechanical equilibrium with no shear stress on the walls. [For the present purposes we define the shear stress, more precisely the (z,x) element of the stress tensor, τ_{zx}, as the x component of the force exerted by the pore fluid on a unit area of wall 2, whose outward normal points in the positive z direction.] Now, if h is held fixed while wall 2 is slid in the x direction (by changing α), then a transverse force should arise, tending to restore wall 2 to its equilibrium position.

To investigate this hypothesis, we have computed τ_{zx} as a function of α for several values of h, all at fixed μ and T. Because μ is fixed, it is convenient to compute the number of atoms N by means of the grand-canonical ensemble Monte Carlo method and then to use N in a microcanonical

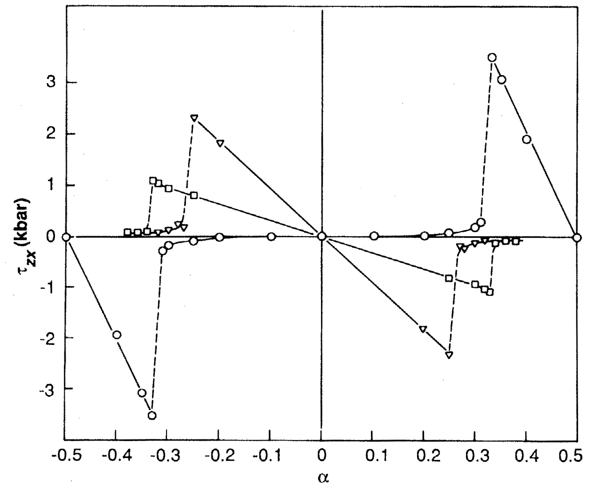

Fig. 2. Shear stress τ_{zx} as a function of strain α for walls separated by $h = 2.20\ \sigma$ (○), $3.10\ \sigma$ (▽), and $4.90\ \sigma$ (□); $\mu/\epsilon = -9.26$; $kT/\epsilon = 1.0$, where k is the Boltzmann constant. Plots correspond to argon, for which $\sigma = 3.405$ Å and $\epsilon = 119.8$ K.

molecular dynamics (MD) calculation at fixed N, h, α, and E, where the total energy E is fixed by adjusting the expected value of the kinetic energy per atom to be consistent with the given temperature according to the equipartition theorem. The advantage of MD is that it allows us to compute dynamic as well as equilibrium properties. In particular, the shear stress is given by

$$\tau_{zx} = F_x^{(2)}/s^2 = \sum_{i=1}^{N} \sum_{j=1}^{N_s} \langle x_{ij} r_{ij}^{-1} du(r_{ij})/dr_{ij} \rangle / s^2 \qquad (3)$$

where s is the side of the unit simulation cell, the brackets signify an average over configurations sampled along the MD trajectory (*12*), and $F_x^{(2)}$ is the total force on wall 2. Because the net force on the walls must vanish, τ_{zx} is also given in terms of the x component of the force on wall 1:

$$\tau_{zx} = -F_x^{(1)}/s^2 \qquad (4)$$

We take the mean of these expressions for τ_{zx}, which differ from one another by less than 1% in all cases. The structure of the pore fluid is characterized in terms of the local density $\rho^{(1)}$ and the in-plane pair correlation function $g^{(2)}$, the computation of which has been described in detail (*8, 9, 12*).

Figure 2 displays plots of τ_{zx} versus α (that is, "stress curves") for three values of h at fixed μ and T; s is fixed at 7.9925 σ and N_s is 50. Because τ_{zx} (and all other properties) must be periodic in the registry α, with a period of unity, we show plots only in the range $-0.5 \leq \alpha \leq 0.5$. By virtue of the symmetry of the walls, τ_{zx} is antisymmetric in α. The shapes of the stress curves are similar, but the curve for $h = 2.20\ \sigma$ differs in phase by $\Delta\alpha = 0.5$ from those for $h = 3.10\ \sigma$ and $4.9\ \sigma$.

For $h = 2.20\ \sigma$ the linear portion of the stress curve is centered on $\alpha = 0.5$, where the walls are fully out of registry and τ_{zx} vanishes exactly. This registry is such that the pore can accommodate just two solid-like layers, each layer containing about 50 atoms (*9*). As the walls are sheared so that α decreases from 0.5, the stress rises approximately linearly with α down to $\alpha \simeq 0.33$, tending to restore the walls to $\alpha = 0.5$. The number of atoms in the pore remains essentially constant; plots of $\rho^{(1)}$ and $g^{(2)}$ indicate two distorted fcc (100) layers sharply localized in the z direction over this range of α. The stress attains a maximum value at about $\alpha = 0.33$. This is the critical stress (S_c above) required to initiate sliding. If the walls are strained beyond this point, the stress abruptly decreases. Simultaneously N decreases by about 44 as α goes from 0.33 to 0.31. Almost an entire layer of fluid suddenly exits the pore over this range of α. Plots of $\rho^{(1)}$ and $g^{(2)}$ now indicate the presence of a single broad layer of fluid. As α decreases further, N gradually decreases to about 50 at $\alpha = 0$, but throughout the range from 0.33 to 0 the stress acts to push the walls back toward $\alpha = 0.5$. The point $\alpha = 0$ is metastable; any slight displacement tends to return wall 2 to the equilibrium registry $\alpha = 0.5$.

For both $h = 3.10\ \sigma$ and $h = 4.90\ \sigma$, the linear portion of the stress curve is centered on $\alpha = 0$, where the walls are precisely in registry and the stress vanishes. With the walls in registry the pore contains three ($h = 3.10\ \sigma$) or five ($h = 4.90\ \sigma$) distorted fcc (100) solid layers, each comprising about 50 atoms. As wall 2 is forced out of registry, the shear stress increases linearly with α; N does not change and the solid layers remain intact according to plots of $\rho^{(1)}$ and $g^{(2)}$. When wall 2 is strained beyond the critical values of α, N drops sharply. For $h = 3.10\ \sigma$, about 41 atoms leave the pore over the range $\alpha = 0.25$ to 0.27; two broad layers of fluid replace the three solid layers. For $h = 4.90\ \sigma$, only about 35 atoms exit the pore over the transition region $\alpha = 0.33$ to 0.34 just beyond the critical strain. At $\alpha = 0.34$ there are still five layers in the pore. The contact layer remains a distorted fcc (100) plane; the first inner layer retains a trace of fcc character; the innermost layer, which is sparsely populated, is strictly fluidal.

The stress curves have the following features. Both the slope of the linear region (the "force constant") and the critical stress decrease as the number of solid layers increases. However, the range of α over which solid-like behavior persists increases with the number of layers; that is, the critical strain increases with the number of layers. The critical strain per layer is constant at about 0.08. With increasing h, the stress curve becomes flatter. At sufficiently large h, the pore should become mechanically stable at all registries.

The decrease of critical stress with increasing number of layers is also observed experimentally (*13*) and can be rationalized as follows. As the number of layers in the pore increases, the solid-like character of the layers decreases toward the center of the pore and it takes less force to break down the less ordered structure of the inner layers.

In conclusion, the results of our Monte Carlo–MD study support a mechanism, namely, solid-liquid transitions, that may account for the experimentally observed critical stress required to initiate the sliding of solid surfaces separated by a molecularly thin film. It should be borne in mind, however, that our idealized model differs in several respects from the actual experiments. First, and perhaps most important, the walls of the prototype are held a fixed distance apart as they are slid at constant T and μ. This leads to a loss of fluid from the pore. In the experiments (*13, 14*) the normal force on the mica sheets is maintained constant while they are slid. The temperature is also constant. No fluid is lost on sliding, which implies that the number of fluid layers remains fixed, even though the separation of the sheets may vary. Second, for the convenience of periodic boundary conditions, the walls of the prototype are taken to be crystallographically aligned. Although control of relative crystallographic orientation (θ) was lacking in the first shear experiments (*13, 14*), recent modifications of the force-balance apparatus by McGuiggan and Israelachvili (*15, 16*) permit θ to be fixed. Third, the structure of the prototypal walls is commensurate with that of the bulk rare-gas solid, thus promoting epitaxial growth of the pore solid, whereas the structure of the mica sheets used in the experiments bears no particular relation to that of the bulk organic solid. X-ray investigations (*17*) demonstrate the formation of solid-like aqueous layers between the silicate layers of tetrahedrally substituted 2:1 phyllosilicates. However, whether the structurally related mica surfaces used in the shear-response measurements can induce "freezing" of organic liquids remains to be seen.

REFERENCES AND NOTES

1. J. N. Israelachvili and G. E. Adams, *J. Chem. Soc. Faraday Trans. 1* **74**, 975 (1978).
2. J. N. Israelachvili, *Intermolecular and Surface Forces* (Academic Press, London, 1985).
3. ———, *Acc. Chem. Res.* **20**, 458 (1987); ——— and P. M. McGuiggan, *Science* **241**, 795 (1988).
4. L. A. Rowley, D. Nicholson, N. G. Parsonage, *Mol. Phys.* **31**, 365 (1976); *ibid.*, p. 389.
5. J. E. Lane and T. H. Spurling, *Chem. Phys. Lett.* **67**, 107 (1979); *Aust. J. Chem.* **29**, 2103 (1976).
6. F. F. Abraham, *J. Chem. Phys.* **68**, 3713 (1979).
7. I. K. Snook and W. van Megen, *ibid.* **72**, 2907 (1980).
8. M. Schoen, D. J. Diestler, J. H. Cushman, *ibid.* **87**, 5464 (1987).
9. C. L. Rhykerd, Jr., M. Schoen, D. J. Diestler, J. H. Cushman, *Nature* **330**, 461 (1987).
10. S. Toxvaerd, *J. Chem. Phys.* **67**, 5291 (1977); *ibid.* **74**, 1998 (1981).
11. J. J. Magda, M. Tirrell, H. T. Davis, *ibid.* **83**, 1888 (1985).
12. M. Schoen, J. H. Cushman, D. J. Diestler, C. L. Rhykerd, Jr., *ibid.* **88**, 1394 (1988).
13. J. N. Israelachvili, P. M. McGuiggan, A. M. Homola, *Science* **240**, 189 (1988).
14. J. van Alsten and S. Granick, *Phys. Rev. Lett.* **61**, 2570 (1988).
15. P. M. McGuiggan and J. N. Israelachvili, *Chem. Phys. Lett.* **149**, 469 (1988).
16. ———, unpublished data.
17. P. G. Slade, P. A. Stone, E. W. Radoslovitch, *Clays Clay Miner.* **33**, 51 (1985).

18. We thank the Scientific Council of the Höchstleistungsrechenzentrum at Kernforschungsanlage Jülich for a generous allocation of computer time on the CRAY X-MP/416 and H. Morgner for his continued interest in the project. Supported under Department of Energy grant DE-FG02-85ER60310.

17 April 1989; accepted 25 July 1989